

# Piccolo, a Presynaptic Zinc Finger Protein Structurally Related to Bassoon

Steven D. Fenster,\*# Wook Joon Chung,\*#  
Rong Zhai,\*# Claudia Cases-Langhoff,\*# Britta Voss,†  
Abigail M. Garner,† Udo Kaempfer,§ Stefan Kindler,‡  
Eckart D. Gundelfinger,§ and Craig C. Garner\*||

\*Department of Neurobiology  
University of Alabama at Birmingham  
Birmingham, Alabama 35294

†Center for Molecular Neurobiology

‡Institute for Cellular Biochemistry  
and Clinical Neurobiology

University of Hamburg  
D-20246 Hamburg

§Leibniz Institute for Neurobiology

D-39118 Magdeburg  
Federal Republic of Germany

## Summary

Piccolo is a novel component of the presynaptic cytoskeletal matrix (PCM) assembled at the active zone of neurotransmitter release. Analysis of its primary structure reveals that Piccolo is a multidomain zinc finger protein structurally related to Bassoon, another PCM protein. Both proteins were found to be shared components of glutamatergic and GABAergic CNS synapses but not of the cholinergic neuromuscular junction. The Piccolo zinc fingers were found to interact with the dual prenylated rab3A and VAMP2/Synaptobrevin II receptor PRA1. We show that PRA1 is a synaptic vesicle-associated protein that is colocalized with Piccolo in nerve terminals of hippocampal primary neurons. These data suggest that Piccolo plays a role in the trafficking of synaptic vesicles (SVs) at the active zone.

## Introduction

At chemical synapses, the presynaptic bouton is a highly specialized neuronal compartment designed for the rapid and regulated release of neurotransmitter. The most remarkable feature is a region of the plasma membrane called the active zone where synaptic vesicles (SVs) dock and fuse (Landis et al., 1988). Typically, several hundred SVs are localized in the vicinity of the active zone and can be divided into a readily releasable pool of docked SVs and a larger, more distally situated reserve pool (Burns and Augustine, 1995; Pieribone et al., 1995). In recent years, the protein machinery directing the SV cycle was well characterized (Südhof, 1995; De Camilli and Takei, 1996). However, the molecular mechanisms that restrict these events to the active zone remain unknown.

Associated with the active zone is an electron-dense

presynaptic cytoskeletal matrix (PCM) (Landis et al., 1988; Hirokawa et al., 1989; Gotow et al., 1991) that is thought to play a role in maintaining the neurotransmitter release site in register with the postsynaptic reception apparatus, regulating the mobilization of SVs and the refilling of release sites. Mechanistically, the PCM may define sites where SVs fuse and recycle through the clustering of the exo- and endocytotic machinery.

SV cycling is a multistep process that involves vesicle mobilization from a reserve pool, docking at active zones, and calcium-dependent fusion (Südhof, 1995; Hanson et al., 1997). The latter two steps require the formation of a complex composed of the vesicle SNARE VAMP2/Synaptobrevin and two target SNAREs, syntaxin and SNAP-25 (Südhof, 1995; Hanson et al., 1997). In addition, a family of low molecular weight GTPases are likely to be involved in SV cycling with rab3 and rab5 regulating exocytotic and endocytotic events, respectively (Ferro-Novick and Novick, 1993; Hess et al., 1993; Südhof, 1995). Data obtained with *rab3A* knockout mice suggest that rab3A modulates the rate at which SVs become available for release (Geppert et al., 1997; Lonart et al., 1998). Rabphilin-3A and RIM interact with rab3A in a GTP-dependent manner via their zinc finger domains (Shirataki et al., 1993; Wang et al., 1997). While rabphilin-3A is a soluble protein (Shirataki et al., 1993), RIM represents a 180 kDa multidomain PCM component that may be involved in the mobilization of SVs from the reserve to the releasable pool (Wang et al., 1997).

We have identified two additional components of the PCM, called Piccolo and Bassoon. Piccolo is a >420 kDa protein detected in presynaptic terminals (Cases-Langhoff et al., 1996). It is tightly bound to the PCM, requiring harsh conditions for extraction. Additionally, immunogold electron microscopy studies indicate that Piccolo is part of the amorphous material (the PCM) situated between SVs located just proximal to the active zone (Cases-Langhoff et al., 1996). Bassoon is a 420 kDa multidomain protein containing two N-terminal zinc finger domains, several coiled-coil domains, and a CAG expansion at its C terminus (tom Dieck et al., 1998). It is exquisitely localized at the neurotransmitter release site of conventional excitatory and inhibitory synapses (tom Dieck et al., 1998; Richter et al., 1999) as well as at the base of retinal ribbon synapses (Brandstaetter et al., 1999).

To gain further insights into the function of the PCM, we determined the primary structure of Piccolo, showing that it is a multidomain zinc finger protein structurally related to Bassoon. Colocalization studies reveal that Piccolo and Bassoon are shared components of both glutamatergic and GABAergic synapses but not neuromuscular junctions. Despite their similarity to the corresponding domains in RIM and rabphilin-3, Piccolo zinc fingers do not interact with rab3A but bind PRA1, a rab3A and VAMP2/Synaptobrevin II-interacting molecule (Martincic et al., 1997; Bucci et al., 1999). These data demonstrate that PCM components are multidomain scaffold proteins likely to be involved in SV cycling at nerve terminals.

|| To whom correspondence should be addressed (e-mail: garner@nrc.uab.edu).

# These authors contributed equally to this work.

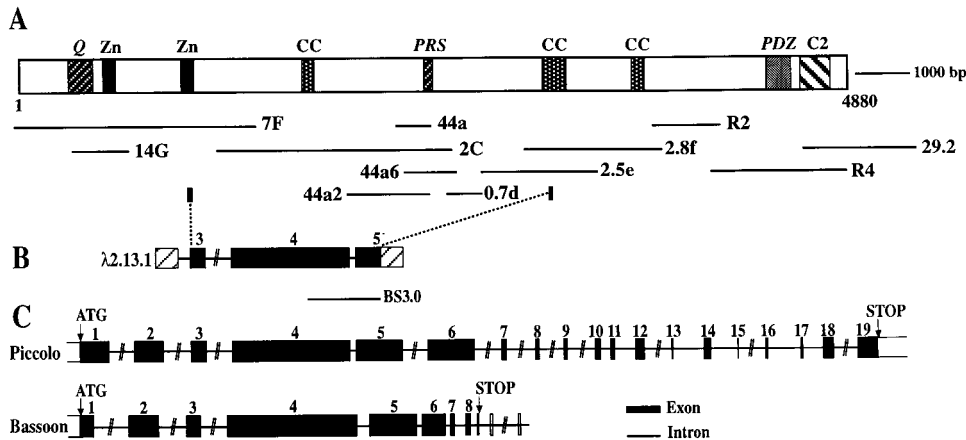


Figure 1. Domain Structure of Piccolo and the Piccolo Gene (*PCLO*)

(A) Domain structure of rat Piccolo as deduced from the analysis of a series of overlapping cDNA clones. Marked domains include: Q, glutamine-rich heptad repeat; Zn, zinc finger; PRS, proline rich sequence; CC, coiled-coil domain; PDZ, PDZ domain; and C2, C2 domain. (B) Mouse genomic clone λ2.13.1 was isolated with clone 44a2 as a radiolabeled probe. The segment of the mouse genomic DNA used to isolate cDNA sequences 3' of clone 44a6 (BS3.0) is also marked. Mouse genomic DNA sequences in clone λ2.13.1 were also used to generate PCR primers to isolate and characterize cDNA clone 0.7d to link 5' and 3' rat Piccolo cDNA clones. Dashed lines indicate the relative position of individual Piccolo domains and the mouse Piccolo exons 3–5. (C) Exon–intron organization of the human *piccolo* gene (*PCLO*). Protein coding region is indicated by closed boxes and 3' untranslated by open boxes. Double slashed lines indicate large gaps in genomic sequence. For comparison, the mapped exon–intron organization of human *bassoon* gene (*BSN*) (Winter et al., 1999) is aligned with Piccolo genomic structure.

## Results

### Piccolo Is a Zinc Finger Protein Structurally Related to Bassoon

In a previous study, designed to isolate structural components of synaptic junctions, a number of cDNA clones encoding novel proteins were identified (Langnaese et al., 1996). Antibodies raised against the coding region of one clone, sap44a, were found to react with a protein of >420 kDa on Western blots that could be localized to the PCM assembled at the active zone of asymmetric type 1 glutamatergic synapses (Cases-Langhoff et al., 1996). The sap44a clone was used to isolate a series of overlapping rat brain cDNA clones spanning the entire protein coding region (Figure 1A). To overcome difficulties in obtaining contiguous cDNA clones, we also isolated λ phages containing regions of the murine *piccolo* gene (Figure 1B). A comparison of DNA sequences made available through the Human Genome Project with the rat Piccolo cDNA sequence allowed us to characterize the exon–intron organization of the human *piccolo* gene (*PCLO*) (Figure 1C). Human *PCLO* has at least 19 exons and spans over 350 kb (Table 1). Interestingly, over half of the cDNA sequence is contained on three large exons (exon 4 [5.1 kb], exon 5 [2.0 kb], and exon 6 [2.1 kb]). The 3' end of the gene contains a number of small exons varying in length from 27 to 231 nucleotides. The 5' end of the gene has not yet been sequenced. A comparison of the coding regions of Piccolo and Bassoon cDNAs revealed a high level of sequence similarity (see below). Moreover, the intron–exon structure of both genes is very similar (Figure 1C and Table 1) (Winter et al., 1999). This observation suggests that the *PCLO* and *BSN* genes evolved by gene duplication. The human *BSN* gene locus has been mapped to 3p21 (Hashida et al., 1998; Winter et al., 1999) and found in mouse to contain

CAG expansion seen in Huntingtin and ataxin (tom Dieck et al., 1998). In addition, Bassoon transcripts exhibit an elevated expression in multiple systems atrophy (Hashida et al., 1998). Of note in this regard, the human *PCLO* gene maps to chromosome 7q11.23–q21.1. This lies very close to a large chromosomal deletion at 7q11.23 that is associated with Williams syndrome (Meng et al., 1998), a genetic disorder associated with a number of pathological features including mental retardation (Morris et al., 1988).

As deduced from the rat nucleotide sequences, Piccolo consists of 4880 amino acid (aa) residues and has a calculated  $M_r$  of ~530 kDa and an isoelectric point (pI) of 6.0 (Figure 2). This is consistent with our earlier studies showing that Piccolo is encoded by a 16 kb transcript and migrates as a >420 kDa protein. The 5'-most cDNA sequence contains a consensus initiation site for translation (Kozak, 1987) with upstream stop codons located in all three reading frames. The human genomic sequence and a brain-specific EST (KIAA0559) (Nagase et al., 1998) allowed the deduction of nearly the entire human Piccolo protein sequence (Figure 2). The overall sequence identity between rat and human Piccolo is 86%. Additionally, Piccolo and Bassoon possess very similar amino acid sequences. Ten regions of homology (50%–80% identity), referred to as Piccolo–Bassoon homology (PBH) regions, were identified (Figure 2). PBH1 and PBH2 are tandem repeats predicted to contain two double zinc finger motifs (aa 519–579 and aa 1010–1066). The Piccolo zinc fingers are 68% identical to each other and 64% identical to those in Bassoon (Figure 3A). In a number of transcription factors and cytoskeletal proteins, zinc fingers have been shown to be sites of protein–DNA and protein–protein interaction, respectively (Sanchez-Garcia and Rabbitts, 1994). The Piccolo/Bassoon zinc fingers are most similar to

Table 1. Exon-Intron Boundaries of Human *PCLO* Gene

Exon Number	Encoded Protein Domain	Exon Size (bp)	5' Splice Donor	Intron Size	3' Splice Acceptor
1	Q, Zn1	—		>16.7 kb	ttatattgtagGTA AAAAGAGT
2	Zn1, Zn2	1407	TTTGACTGAGgtaagttatata	>214.5 kb	tttccccacagATTC AAGAAT
3	Zn2	717	AGAAAAACAgtaagttaaat	8.8 kb	ccctgcttagGAAAAGGAAG
4	CC 1	5080	GTTACTACAGgtcagatgat	364 bp	tgtatttcagCTGAGGTAAT
5	CC 2	2015	GGGCTATACGgtaagagtgat	32.6 kb	ttgattatagACTAAAGGTT
6	CC 3	2182	ATGTCAGACAgtaaggtaaa	5.7 kb	gtgtcccaagCCTATCATCT
7	—	137	TCAAGAGCAAgtaagtgctat	6.1 kb	tatgtcttagATTATACAGA
8	—	91	ACAGTTTCAGgtaaaagcaaat	>12.5 kb	GTAATGGATT
9	PDZ	126	CTTATGGAAG	>5.8 kb	gtctttctagGGATGCAAGT
10	PDZ	109	GTGTAAGACTgtgagttttt	506 bp	taatttttagGGACCTCAAT
11	—	68	C AAAAGCTGgtaggtaaaa	1.1 kb	tttgtttagTGGATAAGGC
12	—	215	CAGCAGCAAGgtcaggttg	3.8 kb	aatattacagCTCAGCGATG
13	—	51	AGAAATTCAGgtatgaagtt	3.1 kb	tctcctaaagCTTCAAATTA
14	C2	125	CAGGGAGAGgtaagtaaaa	2.5 kb	atcaatgcagTCAAGTCATG
15	C2	27	AGAATGCAAGgtagagttgt	7.7 kb	cccaattcagTGCTGAGTAC
16	C2	94	ACTGGAACAGgtatgtcaag	1.2 kb	aactatatagCTCAAGAAAGA
17	C2	72	CCTTGGGGAGgtaagcctct	2.2 kb	tttttttcagGTATTGATTG
18	C2	181	CCATCAAAGgtaggaaata	1.5 kb	ttgtgaccagACATGCAGGT
19	stop codon, 3' UTR	231+	AAAGACGCCAA 3' UTR		

Exon sequences are in capital letters; intron sequences are in lowercase letters; boldface letters indicate consensus splice junctions; blank regions represent gaps in the human genome project. Q, glutamine heptad repeats; Zn-1, Zn-2, double zinc finger motifs; CC1-3, coiled-coil domains; C2, C2 domain; PDZ, PDZ domain. Human genomic sequence was obtained from three genomic clones of 165, 143, and 98 kb in length (DJ0828B12, DJ0784G16, and DJ0897G10).

those found in rabphilin-3A and RIM (40% and 39% similarity, respectively) (Figure 3A). PBH4, 6, and 8 are likely to form coiled-coil structures commonly seen as sites of homo- or heterodimerization (Lupas, 1996). The remaining PBH regions share no similarity with known proteins. At the C terminus, Piccolo contains a single PDZ and C2 domain. These features, absent in Bassoon, are shared with RIM and a brain-specific EST (KIAA0751) (Nagase et al., 1998) we refer to as Oboe, which contain a single PDZ and two C2 domains (Figure 3D). The Piccolo PDZ domain appears to be of the class I type (Daniels et al., 1998) and is most similar to PDZ stretches in RIM and Oboe (Figure 3B). The Piccolo C2 domain, in contrast to those in RIM and Oboe, contains all the consensus aspartate residues required for calcium binding (Figure 3C), indicating that Piccolo may respond to changing calcium levels in nerve terminals. Piccolo also contains a number of proline-rich segments, including one with a stretch of ten prolines from aa 2355–2364 and two putative WW domain-binding motifs (PPXY or PPLP, where X represents any amino acid) from aa 2370–2374 and aa 2381–2384 (Figure 2). Upstream of the PBH1 region are twelve copies of a degenerated decapeptide in tandem array. This region (rich in glutamine and therefore called the Q domain) contains no significant homology to any known protein (Figure 3D). These data demonstrate that Piccolo and Bassoon are structurally related multidomain proteins of the PCM and suggest that they perform a scaffold function mediated through multiple putative protein interaction motifs. Furthermore, Piccolo and Bassoon appear to define a newly emerging gene family that also includes RIM and Oboe as more distantly related members (Figure 3E). Interestingly, analysis of database sequences failed to identify *Caenorhabditis elegans* homologs of Piccolo or Bassoon based on the presence of PBH regions. However, two sequences were found that contain C-terminal PDZ

and C2 domains and seem to represent RIM (Wang et al., 1997) and Oboe homologs (Accession number U70852.1). This suggests that functions performed by multiple family members at vertebrate synapses are performed by only two proteins in *C. elegans*.

#### Piccolo and Bassoon Are Shared Components of Glutamatergic and GABAergic Synapses

Our previous studies on the subsynaptic localization of Piccolo in adult rat brain showed that it is highly restricted to the PCM assembled at the active zone of asymmetric type 1 synapses (Cases-Langhoff et al., 1996). The homology observed between Piccolo and Bassoon (Figure 2) suggests that they may perform analogous functions at different synapses or distinct functions at identical synapses. To test this hypothesis, we examined whether Piccolo colocalizes with Bassoon at different types of synapses. This was accomplished by performing double-label immunofluorescence microscopy of primary neuronal cultures with a collection of antibodies against synaptic proteins. Initially, we compared the distribution of Piccolo and synaptotagmin (a synaptic vesicle protein) in hippocampal neurons cultured for 24 days in vitro (DIV). Approximately 95% of the synaptotagmin immunopositive clusters were observed to colocalize with Piccolo-containing clusters situated along dendritic profiles (Figures 4A–4C). This pattern suggests that Piccolo in these cultures has become localized to synaptic boutons. Double labeling neurons with Piccolo and Bassoon antibodies revealed near one-to-one distribution patterns (Figures 4D–4F), indicating that both PCM proteins are present at identical synapses. To investigate whether Piccolo is present at both excitatory and inhibitory synapses, we compared the distribution of Piccolo to AMPA (GluR1 subunits) and GABA<sub>A</sub> receptors. About 80% and 20% of the Piccolo clusters colocalized with GluR1 and GABA<sub>A</sub>





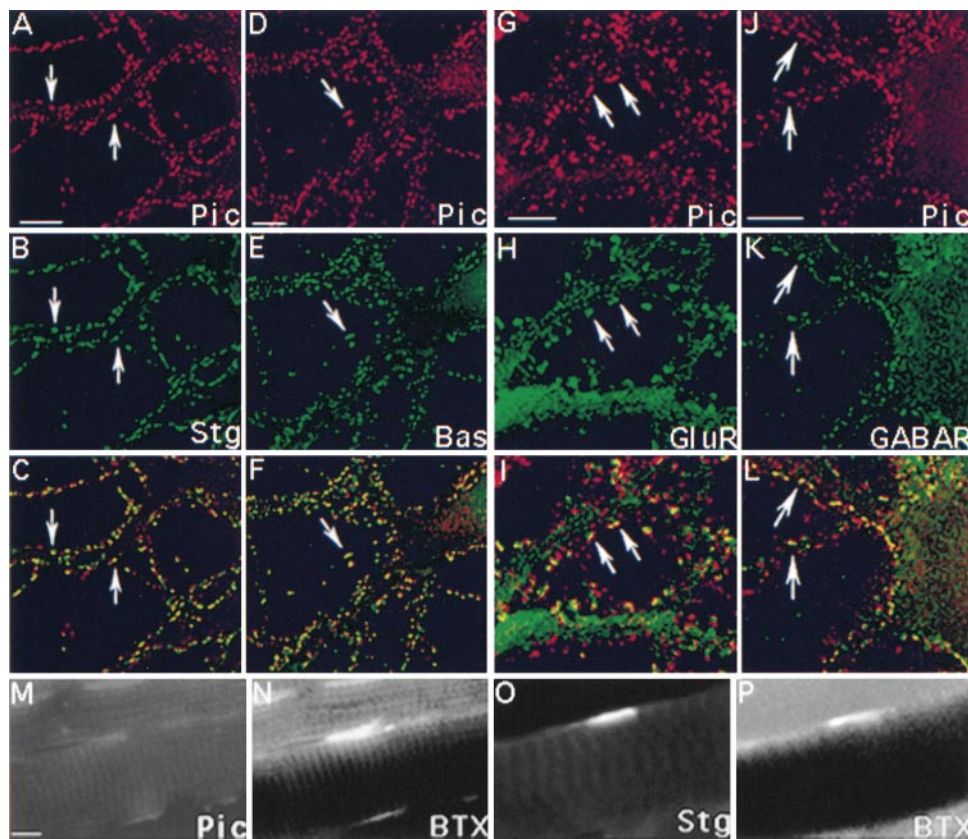


Figure 4. Localization of Piccolo at Various Types of Synapses

(A–L) Rat hippocampal neurons cultured for 24 DIV were double stained with anti-Piccolo (A, D, G, and J), anti-synaptotagmin (B), anti-Bassoon (E), anti-GluR1 (H), or anti-GABA<sub>A</sub> antibodies (K). Merged images for each pair are shown in (C), (F), (I), and (L), respectively. Arrows point to examples of colocalizing clusters. Approximately 95% and 99% of the Piccolo (Pic) clusters (A and D) are observed to colocalize with synaptotagmin (Stg) (C) and Bassoon (Bas) (E) clusters along dendritic profiles, respectively. Piccolo clusters (G) are also observed to colocalize with GluR1 (GluR) subunits of the AMPA receptor at axodendritic and axospinous synapses. Piccolo (J) clusters are also colocalized with GABA<sub>A</sub> Receptor (GABAR) (K) clusters at axodendritic and axosomatic synapses.

(M–P) Longitudinal sections of P7 rat diaphragm stained with FITC-conjugated  $\alpha$ -bungarotoxin (BTX) (N and P) and anti-Piccolo (M) or anti-synaptotagmin (O) antibodies. Scale bars, 20  $\mu$ m.

and Bassoon may interact with rab3A in a GTP-dependent manner. Thus, we used an ELISA-based assay to examine whether the zinc fingers of Piccolo (Pic-Zn1, Pic-Zn2) interact with rab3A in the presence of GDP or GTP $\gamma$ -S. Whereas Pic-Zn1 and Pic-Zn2 did not bind under either condition, a robust interaction of the rabphilin-3A zinc finger (Rabp-Zn) with rab3A was seen in the presence of GTP $\gamma$ -S (data not shown). These results were confirmed in a yeast two-hybrid assay. Only yeast doubly transfected with rab3A and Rabp-Zn were able to grow on plates lacking histidine and turned blue in 30 min when incubated with X-gal (Figure 5A). The Pic-Zn1 bait construct was self-activating and could not be tested in this assay.

Subsequently, we employed Pic-Zn2 as a bait in a yeast two-hybrid screen to identify potential interacting partners. Screening  $3 \times 10^6$  transformants yielded seven independent clones interacting with Pic-Zn2. Two clones encoded PRA1, a small 21 kDa protein originally identified through its interaction with rab3A (Martincic et al., 1997; Bucci et al., 1999). To confirm this interaction, we compared the specificity of PRA1 for the zinc fingers from rabphilin-3A (Rabp-Zn) or Piccolo Zn2. As

shown in Figure 5A, PRA1 could interact with Pic-Zn2 but not Rabp-Zn. To assess whether PRA1 binding is specific for either of the Piccolo zinc fingers, we performed an overlay assay using His<sub>6</sub>-PRA1 as a probe to assay binding to immobilized GST-tagged zinc finger fusion proteins. As seen in Figure 5B, His<sub>6</sub>-PRA1 interacted with both GST-Pic-Zn1 and GST-Pic-Zn2, but not with GST-Rabp-Zn or GST. It should be noted that although GST-Pic-Zn2 was significantly degraded (Figure 5C, lane 4), His<sub>6</sub>-PRA1 still bound the full-length molecule. These results indicate that the inability of the Piccolo zinc fingers to interact with rab3A is not due to incorrect domain folding but represents a different binding specificity as compared to Rabp-Zn.

One of the characteristics described for the association of PRA1 with its SV binding partner, VAMP2/Synaptobrevin II, is a sensitivity to (0.1%) Triton X-100 (Martincic et al., 1997). To assess whether PRA1 binding to the Piccolo zinc fingers shares this feature, an ELISA-based assay was used to determine the relative binding affinity of PRA1 for Pic-Zn1 in the presence and absence of Triton X-100. As seen in Figure 5D, His<sub>6</sub>-PRA1 bound GST-Pic-Zn1 in a concentration-dependent manner but

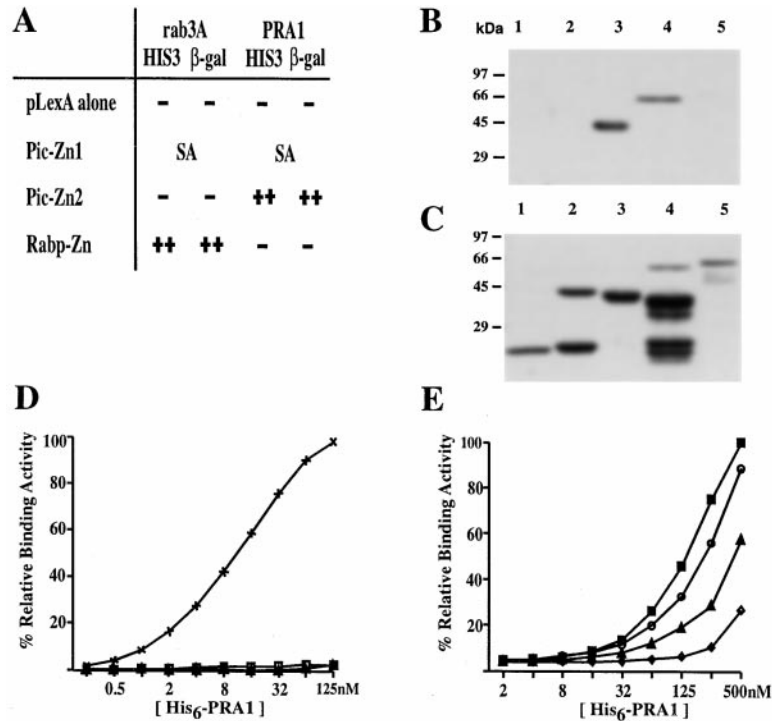


Figure 5. In Vitro Binding of Piccolo Zinc Fingers with PRA1

(A) Yeast two-hybrid assay assessing binding of PRA1 and rab3A to the Piccolo (Pic-Zn2) and rabphilin-3A (Rabp-Zn) zinc finger domains. Interactions between these constructs are indicated by pluses (+), as measured by the ability of transfected colonies to induce the reporter genes *His3* and *lacZ*. SA, self-activating.

(B and C) Filter overlay assay showing direct binding of PRA1 to the Piccolo zinc fingers. Purified GST fusion proteins were separated by SDS PAGE and stained with Coomassie Blue (C) or transferred to nitrocellulose (B). Lane 1, GST alone; 2, GST-C2A (C2A domain of Piccolo); 3, GST-Pic-Zn1 (Piccolo); 4, GST-Pic-Zn2 (Piccolo); 5, GST-Rabp-Zn (rabphilin-3A). Binding of purified His<sub>6</sub>-PRA1 was visualized by immunoblotting with anti-T7 Tag antibody (B). The positions of the molecular weight standards are indicated in kilodaltons.

(D) ELISA binding assay demonstrating the ability of PRA1 to interact specifically with the Piccolo zinc fingers. GST-zinc finger fusion proteins (50 pmol) were bound to the 96-well plate and then incubated with increasing concentrations of His<sub>6</sub>-PRA1. Percent binding of His<sub>6</sub>-PRA1 to the first Piccolo zinc finger (GST-Pic-Zn1, crosses), the rabphilin-3A zinc finger domain (GST-Rabp-Zn, closed triangles), or the Piccolo C2A domain (GST-C2A, open squares) was normalized against the maximal binding of His<sub>6</sub>-PRA1 to GST-Pic-Zn1.

(E) Detergent sensitivity of PRA1 binding to Pic-Zn1 in 0.01% Triton X-100 (closed squares), 0.05% Triton X-100 (open circles), 0.1% Triton X-100 (closed triangles), and 0.5% Triton X-100 (open diamonds). Percent binding was normalized against the maximal binding of GST-Pic-Zn1 with His<sub>6</sub>-PRA1 in the presence of 0.01% Triton X-100. Note even low levels of Triton X-100 dramatically affect PRA1 binding to Piccolo (compare to [D]).

not GST-Rabp-Zn. In contrast, PRA1 binding to GST-Pic-Zn1 was almost completely abolished in 0.1% Triton X-100 (Figure 5E). Significant degradation of GST-Pic-Zn2 (see Figure 5C) did not permit a quantitative measure of its binding affinity. Nonetheless, when 0.1% Triton X-100 was added to the overlay assay, binding of PRA1 to the second zinc finger was also abolished (data not shown). These results demonstrate that PRA1 associates with the Piccolo zinc fingers in vitro and that this interaction is detergent sensitive as observed for VAMP2/Synaptobrevin II binding to PRA1 (Martincic et al., 1997).

#### PRA1 Colocalizes with Piccolo in Nerve Terminals

To investigate whether the interaction of PRA1 with Piccolo may be of significance in vivo, we compared the spatial distribution of Piccolo and PRA1 in cultured hippocampal neurons. PRA1 exhibits a generally diffuse staining pattern throughout the neuronal processes in contrast to the distinct punctate pattern of Piccolo (Figure 6A). However, clusters of PRA1 immunoreactivity colocalize with Piccolo clusters along dendritic profiles, indicating that PRA1 is also present at synapses. This conclusion is supported by the codistribution of PRA1- and synaptotagmin-immunoreactive clusters along dendritic profiles (Figure 6A).

The synaptic localization of PRA1 and its ability to interact in vitro with VAMP2/Synaptobrevin II, prenylated rabs (Martincic et al., 1997), and Piccolo raises the question of whether PRA1 in nerve terminals can

associate with SVs or the PCM or both. Despite its vesicular protein binding partners, it has not been reported whether PRA1 actually associates with SVs. Therefore, we examined whether PRA1 is present in synaptosomes and whether it can physically interact with SVs. Figure 6B shows a Western blot of rat brain synaptosomes stained with PRA1 antibodies. PRA1 and its interacting partners, rab3A and VAMP2/Synaptobrevin II, were present in this cellular fraction (Figure 6B). To assess whether PRA1 is associated with SVs, we performed a flotation assay with lysed synaptosomes. Similar to synaptophysin, PRA1 immunoreactivity was found in the 0.3 M sucrose fraction, indicating that PRA1 is associated with SVs (Figure 6C). This was confirmed by immunoprecipitation experiments using synaptophysin antibody-coated beads. In the bound fraction, PRA1 was affinity purified along with synaptophysin, rab3A and VAMP/Synaptobrevin II (Figure 6D). No immunoreactivity was detected when a goat anti-mouse IgG was coupled to the bead. These data strongly indicate that PRA1 is a component of SVs and is poised to interact with Piccolo in presynaptic nerve terminals.

To assess whether PRA1 may also be associated with the PCM, we compared the partitioning of PRA1 and Piccolo into synaptosomal, synaptic plasma membrane, and detergent-extracted synaptic junctional (PSD) preparations. Whereas Piccolo is present in all three preparations, PRA1 is only found in the synaptosomal and synaptic plasma membrane fractions (Figure 6B). The absence of PRA1 from the PSD preparation indicates

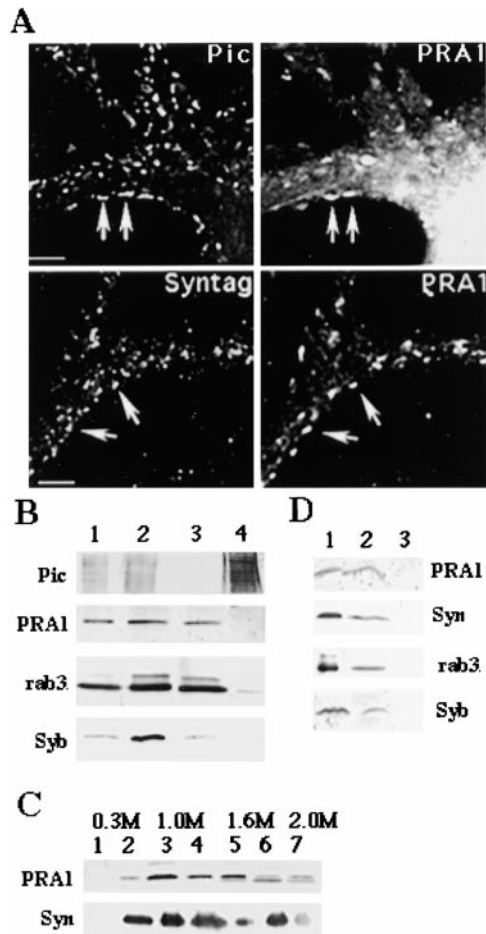


Figure 6. PRA1 Is Present in Nerve Terminals and Associated with SVs

(A) Hippocampal neurons cultured for 24 DIV were stained with antibodies against PRA1 and Piccolo (Pic) or synaptotagmin (Syntag). PRA1 clusters are found colocalized with Piccolo and synaptotagmin clusters along dendritic profiles (arrows). Scale bars, 20  $\mu$ m. (B) Fractionation of synaptosomes. Synaptosomes (1), synaptic plasma membranes (2), supernatant (3), and pellet (4) of Triton X-100 extracted synaptic plasma membrane fractions were separated by 5%–15% gradient SDS-PAGE and immunoblotted with antibodies against Piccolo (Pic), PRA1, rab3A/C (rab3), or VAMP2/Synaptobrevin II (Syb). Multiple bands detected with the Piccolo antibody represent some proteolysis of 530 kDa Piccolo. Note equal amounts of protein were loaded in each lane.

(C) Flotation assay of lysed synaptosomal membranes. Gradient fractions were separated by SDS-PAGE and Western blotted with PRA1 and synaptophysin (Syn) antibodies. Lanes 1–7 represent 0.5 ml fractions from the 0.3–2.0 M sucrose gradient.

(D) Immunoprecipitation of SVs. Beads coated with anti-synaptophysin antibodies or goat anti-mouse IgG were incubated with the light membrane fraction (0.3–1.0 M sucrose fractions in [C]) from the lysed synaptosome preparation. Proteins in input (lane 1), proteins bound to synaptophysin antibody-coated beads (lane 2), and proteins bound to IgG-coated beads (lane 3) were separated by SDS-PAGE and Western blotted with antibodies against PRA1, synaptophysin (Syn), rab3A/C (rab3), and VAMP2/Synaptobrevin II (Syb).

that its association with the synaptic junction is detergent sensitive. A similar detergent sensitivity has also been observed in the binding of PRA1 to all of its known binding partners, including rabs, VAMP2/Synaptobrevin

II (Martincic et al., 1997), and the Piccolo zinc fingers (Figure 5). This feature as well as the harsh detergent conditions required to solubilize Piccolo from rat brain synaptic junctional preparations (Cases-Langhoff et al., 1996) makes it unfeasible to use immunoprecipitation to prove that Piccolo and PRA1 interact in vivo. Nonetheless, the ability of PRA1 to interact with the Piccolo zinc fingers in three different in vitro binding assays, to associate with SVs, and to colocalize with Piccolo in nerve terminals strongly suggests that the Piccolo-PRA1 interaction is of functional relevance for SV trafficking at the presynaptic plasma membrane.

## Discussion

To characterize the molecular machinery that defines the PCM, we have determined the structure of Piccolo, a novel presynaptic multidomain zinc finger protein. Piccolo is a member of a newly emerging family of PCM proteins that includes Bassoon and RIM. In addition, we have used a series of in vitro binding assays to show that in contrast to RIM, the zinc fingers in Piccolo do not bind directly to rab3A but to the rab3-VAMP2/Synaptobrevin II-interacting protein PRA1. These data raise the possibility that Piccolo participates in the recycling of SVs in nerve terminals.

The docking, fusion and recycling of vesicles in nerve terminals are features common to all chemical synapses. Nonetheless, synapses are morphologically distinct. For example, in contrast to the smooth presynaptic morphology of type 1 and 2 synapses, photoreceptor cells, synapsing onto bipolar cells and horizontal cells in the retina, have presynaptic ribbons along which SVs are tethered (Boycott and Kolb, 1973). Our previous data and the results presented here show that Piccolo is a component of the PCM assembled at both type 1 glutamatergic and type 2 GABAergic synapses. More recently, we have found Piccolo at ribbon synapses in the retina (C. C.-L. and C. C. G., unpublished data). In addition, the PCM protein Bassoon is also present at both excitatory and inhibitory synapses as well as the ribbon synapse (tom Dieck et al., 1998; Brandstaetter et al., 1999; Richter et al., 1999). Here, we show that Piccolo and Bassoon cocluster at synaptic boutons in primary hippocampal neurons. These data imply that both proteins are present at identical synapses. Moreover, their structural similarity suggests that Piccolo and Bassoon perform partially overlapping functions at a variety of structurally and functionally diverse synapses. Experiments designed to disrupt the Piccolo and Bassoon genes will help to unravel the cellular functions of both proteins.

Although the overall genomic and protein structures of Piccolo and Bassoon are very similar, there are some clear differences. Situated at the C terminus of Piccolo, but absent in Bassoon, are a PDZ and a C2 domain. This combination of domains is also observed in RIM (Wang et al., 1997) and Oboe, which both contain a single PDZ and two C2 domains. PDZ domains were originally identified in the MAGUK family of scaffold proteins as well as in a growing number of cortical cytoskeletal proteins that direct the assembly of macromolecular signaling complexes (Garner and Kindler, 1996). PDZ

domains interact with proteins containing a C-terminal T/SXV motif such as voltage- and ligand-gated ion channels as well as cell adhesion molecules (Craven and Brecht, 1998). This suggests that the PDZ domains in Piccolo and RIM may interact with proteins at the active zone plasma membrane. This may act to localize these PCM proteins and position their C2 domains near calcium entry sites through voltage-activated N-type calcium channels. C2 domains, first identified in PKC, are  $\text{Ca}^{2+}$ /phospholipid binding elements found in a number of synaptic proteins (Südhof and Rizo, 1996). In synaptotagmin, calcium in a 20–100  $\mu\text{M}$  range regulates the interaction of its C2 domains with syntaxin during the SV fusion step (Sugita et al., 1996). C2 domains are characterized by five conserved aspartate residues involved in  $\text{Ca}^{2+}$  binding. These residues are conserved in the Piccolo C2 domain, suggesting that calcium influx through N-type calcium channels at the active zone may regulate the biological activity of Piccolo. Piccolo also contains a number of proline-rich regions, which could serve as ligands for SH3 and WW domain-containing proteins. Many of the proteins implicated in endocytosis such as amphiphysin (David et al., 1996), the SH3p4/SH3p8/SH3p13 family (Ringstad et al., 1997), intersectin (Yamabhai et al., 1998), dap160 (Roos and Kelly, 1998), and Syndapin (Qualmann et al., 1999) contain one or more SH3 domains and could possibly interact with proline-rich regions of Piccolo in nerve terminals. The multidomain structure and restricted localization of Piccolo at sites of neurotransmitter release and vesicle recycling give compelling evidence that Piccolo could serve as a presynaptic scaffold protein on which components of SV endo- and exocytosis can be specifically sequestered in the presynaptic nerve terminal.

Our studies on the zinc finger domains in Piccolo provide evidence that the PBH regions are sites of protein-protein interaction. The Piccolo and Bassoon zinc finger domain (PBH1 and PBH2) are 65% identical and ~40% and 39% similar to the single zinc fingers present in rabphilin-3A and RIM, respectively. The latter have been shown to bind rab3A in a GTP-dependent manner, suggesting a role for these proteins in vesicle trafficking at nerve terminals. The association of RIM with the PCM (Wang et al., 1997) suggests a potential role for RIM in regulating the mobilization of SVs from the reserve to the release-ready pool. Recent work on the crystal structure of the rab3A complex with the effector domain of rabphilin-3A suggests that a SGAWFF motif flanking the rabphilin-3A zinc finger is required for rab3A binding. A similar motif is found adjacent to the rab3A binding zinc finger in RIM (Ostermeier and Brunger, 1999) but is not present in the sequences flanking the zinc fingers in Piccolo and Bassoon. This is consistent with our finding that Piccolo zinc fingers do not bind rab3A. However, given the inability of Noc2 to bind rabs (Kotake et al., 1997), clearly the presence or absence of this motif is not sufficient to conclude a priori whether rabs will bind a given zinc finger.

Piccolo zinc fingers, but not the corresponding domains in rabphilin-3A, specifically interact with the rab3A-VAMP2/Synaptobrevin II effector PRA1 in different *in vitro* assay systems. A direct interaction between PRA1 and Piccolo *in vivo* could not be demonstrated

due to the detergent sensitivity of PRA1 binding to Piccolo. The detergent sensitivity is also observed in the interaction between PRA1 and rab3A or VAMP2/Synaptobrevin II (Martincic et al., 1997). Structurally, this appears to be related to the presence of two hydrophobic regions in PRA1 that participate in prenylated rab and VAMP2/Synaptobrevin II binding (Martincic et al., 1997). Presumably, the presence of detergent changes the conformation of PRA1 and effects its binding to the Piccolo zinc fingers. Nonetheless, the association of PRA1 with SVs, its presence in synaptosomal and synaptic plasma membrane preparations, its colocalization with Piccolo in nerve terminals, and its ability to interact with Piccolo *in vitro* support the hypothesis that PRA1 can interact with Piccolo at the active zone. In view of PRA1's interaction with two fundamentally diverse protein families involved in vesicle trafficking, i.e., rabs and VAMP2/Synaptobrevin II, it has been speculated that PRA1 may play a role in regulating the interaction of VAMP2/Synaptobrevin II with t-SNARE components (Martincic et al., 1997; Bucci et al., 1999). Alternatively, PRA1 may also affect the ability of rabs to interact with their effectors. If this is the case, a transient association of PRA1 with Piccolo in the PCM could serve to unmask rab3A and/or VAMP2/Synaptobrevin II on SVs. This would allow rab3A to interact with the PCM protein RIM in a GTP-dependent manner and VAMP2 to interact with syntaxin and SNAP-25 to initiate the formation of the SNARE docking complex at the active zone.

In conclusion, we have described a novel component of the PCM, Piccolo, that is localized in the presynaptic nerve terminals of both excitatory and inhibitory synapses in CNS. Our analysis of the primary structure of Piccolo has revealed that it is a multidomain protein structurally related to Bassoon. Both are members of a newly emerging family of proteins likely to be involved in the cycling of SVs in nerve terminals.

## Experimental Procedures

### Primary Antibodies

Piccolo mouse and rabbit polyclonal antibodies generated against sap44a and 44a2 sequences, respectively, fused to GST were prepared and affinity purified as previously described (Cases-Langhoff et al., 1996). The Bassoon monoclonal antibody was used as described previously (tom Dieck et al., 1998). The mouse monoclonal antibodies against synaptotagmin, VAMP2/Synaptobrevin II, and rab3A/C were kindly provided by Dr. R. Jahn (Max-Planck-Institut, Goettingen, Federal Republic of Germany). The rabbit polyclonal antibody anti-GluR1 was purchased from Chemicon. The mouse monoclonal anti-GABA<sub>A</sub> and synaptophysin antibodies were purchased from Boehringer Mannheim. Polyclonal anti-PRA1 rabbit serum was kindly provided by Dr. J. Ngsee (University of Ottawa).

### Preparation of Primary Hippocampal Cultures and Immunofluorescence Microscopy

Primary rat hippocampal cultures were prepared and grown on coverslips as previously described (Ye and Sontheimer, 1998). Cells were fixed and processed for immunofluorescence microscopy as described (tom Dieck et al., 1998). Digital images were taken on a Nikon Diaphot 300 microscope equipped with a Photometric CH250 cooled camera. Images were captured with IP lab spectrum software (Signal Analytics) and presented in Adobe Photoshop (Adobe).

### Immunohistochemistry of Rat Diaphragm

P7 rats were perfused with 4% (w/v) paraformaldehyde in 100 mM phosphate buffer (PB [pH 7.4]). The diaphragm was removed, post-fixed overnight in 2% (w/v) paraformaldehyde-PB, and cryoprotected in 30% (w/v) sucrose in PB (until tissue sinks in the solution

or for a maximum of 48 hr). Tissue was embedded in Tissue-Tek (Miles) and frozen at  $-70^{\circ}\text{C}$ . Diaphragm sections ( $6\ \mu\text{m}$ ) were blocked with 5% (v/v) FCS in PBS for 2 hr and incubated overnight with FITC-conjugated  $\alpha$ -bungarotoxin (Sigma) and rabbit anti-Piccolo antibodies (1:100 dilution), mouse anti-Bassoon antibodies (1:100 dilution), or a mouse antibody against synaptotagmin (1:100 dilution) at  $4^{\circ}\text{C}$  in 5% FCS/PBS. Fluorescent images were collected and processed as described above.

#### Cloning and Sequence Analysis of Rat Piccolo cDNA and Mouse Genomic Clones

The cDNA clone 44a was isolated from a  $\lambda\text{gt}11$  expression library with polyclonal antibodies generated against a rat brain synaptic junctional preparation as described previously (Langnaese et al., 1996). The cDNA clones 2C, 7F, and 44a6 spanning the 5' end of the cDNA sequence were isolated by screening an adult rat cerebellum  $\lambda\text{ZAPII}$  library with  $^{32}\text{P}$ -labeled 44a cDNA by random priming as previously described (Ausubel et al., 1998). The isolation of clones 3' of 44a6 using 44a6 cDNA as a probe from a variety of rat brain cDNA libraries was unsuccessful. This obstacle was overcome by using 44a2 cDNA as a radiolabeled probe to isolate mouse genomic clones from a 129 SVJ  $\lambda\text{FIXII}$  library (Stratagene) containing exons encoding 3' Piccolo sequence. A 3.0 kb BamHI/Sall genomic fragment (BS3.0) from mouse clone  $\lambda\text{2.13.1}$ , hybridizing to 44a6 and 44a on a Southern blot, was gel purified as described (Qiagen) and subcloned into pBluescript (Stratagene). Oligonucleotides derived from DNA sequence immediately proximal to the 3' end of the 44a6 sequence and the 3' end of the 3.0 kb BamHI/Sall genomic fragment were used to generate a 2.1 kb DNA fragment by polymerase chain reaction (PCR). This fragment was  $^{32}\text{P}$ -labeled and used to screen an adult rat brain stem and spinal cord  $\lambda\text{ZAPII}$  cDNA library (courtesy of Dr. S. Carroll, University of Alabama at Birmingham) to isolate additional 3' cDNA clones. DNA sequences present in the mouse genomic clone but absent in the cDNA clones 44a6 and 2.5e were confirmed to represent Piccolo coding sequence by PCR. In brief, oligonucleotide primers representing 3' 44a6 sequence (GAACCTG GGAAGCTCAACAGA) and 5' 2.5e sequence (CTCGCTACTAGTTCCTGTG) were used to generate a 750 bp DNA fragment from mouse brain cDNA (0.7M) and rat genomic DNA (0.7R). The nucleotide sequence of both genomic DNA and cDNA clones were determined by fluorescent dideoxynucleotide chain termination method with an automated ABI 373 DNA sequencer at the UAB DNA sequencing facility. DNA and protein sequences were analyzed with the GeneWorks program package (Intelligenetics). Human Piccolo amino acid sequence was translated from genomic sequence obtained from three large human genomic clones sequenced by the Genome Sequencing Center at Washington University (Accession numbers AC004903, AC004886, and AC004082). Additional sequence containing the 3' cDNA sequence of human Piccolo was obtained from KIAA0559 (Accession number AB011131), and Oboe sequence was derived from KIAA0751 (Accession number AB018294).

#### Synaptosome Preparation, Flotation Assay, and SV Immunoprecipitation

The isolation of synaptosome, synaptic plasma membrane, and synaptic junctional preparations was performed as described (Cases-Langhoff et al., 1996). Equal amount of proteins from each fraction were separated by a 3%–15% SDS-PAGE, transferred to nitrocellulose membranes (MSI), and immunoblotted with anti-Piccolo, -rab3A, -PRA1, and -VAMP2/Synaptobrevin II antibodies followed by alkaline phosphatase (AP)-conjugated secondary antibodies. The flotation assay was modified from Balch et al. (1984). Briefly, the hypotonically lysed synaptosomal fraction was adjusted to 2.0 M sucrose, loaded to SW60 tube, and overlaid with 1.6 M, 1.0 M, and 0.3 M sucrose layers. The gradients were centrifuged for 3 hr at  $350,000 \times g$  in SW60 rotor. The 0.5 ml fractions were taken from the top to the bottom of the tube, resolved by SDS-PAGE, and blotted for PRA1 and synaptophysin. The light membrane fractions from the 0.3–1.0 M sucrose boundary were incubated with synaptophysin monoclonal antibody or goat anti-mouse IgG-coated M500 beads (Dyna) at  $4^{\circ}\text{C}$  overnight. Beads were collected and washed extensively with 0.1% BSA/PBS (Jin et al., 1996). Proteins in the bound

fractions and the input fractions were analyzed by SDS-PAGE and Western blotting.

#### Construction of Fusion Proteins

The vector pGEX 2T.1 was generated by introducing a pair of complementary oligonucleotides (GATCTCGAGCGGAATTCGTCGACG GATCCGC and AATTGCGGATCCGTCGACGAATTCGCTCGA) into the BamHI/EcoRI site of the pGEX2T.1 vector (Pharmacia). The vector pRSET B1 was generated by introducing a complementary set of oligonucleotides (GATCGAGCTCGAGAAAGCTTCGAATTCGGA TCCGTCGACAC and AGCTGTGTCGACGGATCCGAATTCGAAGCT TTCTCGAGCTC) into the BamHI/HindIII site of the pRSET B vector (Invitrogen). GST-Pic-Zn1 and GST-Pic-Zn2 from Piccolo (Zn1, aa 485–629; Zn2, aa 866–1122) were constructed by amplifying Piccolo cDNA sequence by PCR and subcloning into pGEX 2T.1. GST-Rabp-Zn was constructed by amplifying N-terminal region containing the zinc finger domain (aa 1–281) of rabphilin-3A cDNA (DNA kindly provided by K. Kirk, University of Alabama at Birmingham) by PCR and subcloning into the pGEX2T.1 vector. His<sub>6</sub>-Rab3A was constructed by subcloning full-length rab3A from pGEX-rab3A (DNA kindly provided by K. Kirk, University of Alabama at Birmingham) into the pRSET A vector (Invitrogen). His<sub>6</sub>-PRA-1 was constructed by amplifying full-length PRA1 from a rat brain  $\lambda\text{gt}11$  cDNA library by PCR and subcloning into the pET32a+ vector (Novagen). GST and His-tagged fusion proteins were purified on glutathione agarose beads (Sigma) and Talon metal affinity resin (Clontech), respectively, following the manufacturer's instructions.

#### Yeast Two-Hybrid Screening and Assay

The yeast two-hybrid screen was performed using a mouse brain MATCHMAKER LexA cDNA library (Clontech) with Pic-Zn2 of Piccolo as a bait. The pLexA-Pic-Zn2 bait construct was generated by subcloning the Pic-Zn2 fragment from pGEX-Pic-Zn2 into pLexA. The bait construct and the mouse brain cDNA library in the prey vector were cotransformed into EGY48[p8oplacZ] yeast cells, and positive clones were selected according to the MATCHMAKER protocols (Clontech). The prey plasmids were isolated and cotransformed with either pLexA-Pic-Zn2 or pLexA into EGY48[p8oplacZ] yeast cells to confirm the interaction. The nucleotide sequences of prey plasmids were determined by DNA sequencing at the UAB sequencing core facility.

The pLexA-Pic-Zn1 (aa 485–629), pLexA-Rabp-Zn (aa 1–281), and pB42AD-rab3A were generated from Piccolo, rabphilin-3A, and rab3A cDNA sequences, respectively, by PCR amplification as described above. To examine the interaction between rab3A or PRA1 and the zinc finger domains, the prey construct pB42AD-rab3A or pB42AD-Pic-Zn2/6-5 (PRA1) and each of the bait constructs containing the zinc finger domains were cotransformed into EGY48 [p8oplacZ] yeast cells. Yeast clones cotransformed with bait and prey constructs were selected on plates lacking uracil, histidine, and tryptophan. Positive clones were selected and assayed for His growth and  $\beta$ -galactosidase activity as described in the MATCHMAKER protocols (Clontech).

#### ELISA and Overlay Assay

Interactions of the GST-zinc finger fusion proteins with His<sub>6</sub>-rab3A or His<sub>6</sub>-PRA1 were performed with an ELISA assay as described previously (Kuhlendahl et al., 1998). In brief, for the zinc finger proteins and rab3A interaction, GST fusion proteins were bound to a 96-well plate (Nunc) and incubated with His<sub>6</sub>-rab3A in the presence of 1mM GTP- $\gamma$ -S or GDP (Sigma). His<sub>6</sub>-rab3A bound to the GST fusion proteins was probed with T7 mouse monoclonal antibody (Invitrogen) followed by an AP-conjugated secondary antibody. For the zinc finger domains and PRA1, the GST fusion proteins bound to a 96-well plate were incubated with His<sub>6</sub>-PRA1 in the presence of 0.01%, 0.05%, 0.1%, or 0.5% Triton X-100. The plate was further incubated with an anti-thio antibody (Novagen) followed by an AP-conjugated secondary antibody. The amount of His<sub>6</sub>-tagged proteins bound to the GST fusion proteins was calculated by measuring the colorimetric AP reaction with p-nitrophenyl phosphate at 405 nm using an ELISA plate reader.

For the overlay assay, 100 pmol of GST fusion proteins were separated on 10% SDS-PAGE gel and transferred to nitrocellulose

membrane. The membrane was blocked for nonspecific binding in blocking solution (1× TBS, 5% skim milk, and 0.01% Tween-20) for 30 min, followed by incubation with 0.1 μM His<sub>6</sub>-PRA1 in blocking solution for 1 hr at room temperature. The membrane was further incubated with anti-thio mouse monoclonal antibody (Invitrogen) followed by an AP-conjugated secondary antibody. The His<sub>6</sub>-PRA1 bound to the GST fusion proteins was visualized by the colorimetric AP reaction with nitro blue tetrazolium (NBT) and 5-bromo-4-chloro-3-indoyl phosphate (BCIP).

#### Acknowledgments

We would like to thank S. Lyons, F. Hester, and J. O'Neal for technical assistance; Johnny K. Ngsee for the generous gift of PRA1 antibody; and R. Jahn for providing antibodies against synaptotagmin, synaptobrevin, and rab3a. This work was supported by the Federal Government of Germany (BMBF), the Keck Foundation, grants from the National Institutes of Health (P50 HD32901, AG 12978-02, AG 06569-09) to C. C. G., from the Deutsche Forschungsgemeinschaft (SFB 426/A1, SFB444) to E. D. G. and S. K., and from the Fonds der Chemischen Industrie to E. D. G.

Received July 12, 1999; revised October 26, 1999.

#### References

- Ausubel, F.M., Brent, R., Kingston, R.E., Moore, D.D., Seidman, J.G., Smith, J.A., and Struhl, K., eds. (1998). *Current Protocols in Molecular Biology* (New York: John Wiley and Sons).
- Balch, W.E., Dunphy, W.G., Braell, W.A., and Rothman, J.E. (1984). Reconstitution of the transport of protein between successive compartments of the Golgi measured by the coupled incorporation of N-acetylglucosamine. *Cell* 39, 405–416.
- Boycott, B.B., and Kolb, H. (1973). The connections between bipolar cells and photoreceptors in the retina of the domestic cat. *J. Comp. Neurol.* 148, 91–114.
- Brandstaetter, J.H., Fletcher, E.L., Garner, C.C., Gundelfinger, E.D., and Waessle, H. (1999). Differential expression of the presynaptic cytomatrix protein Bassoon among the ribbon synapses in the mammalian retina. *Eur. J. Neurosci.*, in press.
- Bucci, C., Chiariello, M., Lattero, D., Maiorano, M., and Bruni, C.B. (1999). Interaction cloning and characterization of the cDNA encoding the human prenylated rab acceptor (PRA1). *Biochem. Biophys. Res. Commun.* 258, 657–662.
- Burns, M.E., and Augustine, G.J. (1995). Synaptic structure and function: dynamic organization yields architectural precision. *Cell* 83, 187–194.
- Cases-Langhoff, C., Voss, B., Garner, A.M., Appeltauer, U., Takei, K., Kindler, S., Veh, R.W., De Camilli, P., Gundelfinger, E.D., and Garner, C.C. (1996). Piccolo, a novel 420 kDa protein associated with the presynaptic cytomatrix. *Eur. J. Cell Biol.* 69, 214–223.
- Craven, S.E., and Bredt, D.S. (1998). PDZ proteins organize synaptic signaling pathways. *Cell* 93, 495–498.
- Daniels, D.L., Cohen, A.R., Anderson, J.M., and Brunger, A.T. (1998). Crystal structure of the hCASK PDZ domain reveals the structural basis of class II PDZ domain target recognition. *Nat. Struct. Biol.* 5, 317–325.
- David, C., McPherson, P.S., Mundigl, O., and De Camilli, P. (1996). A role of amphiphysin in synaptic vesicle endocytosis suggested by its binding to dynamin in nerve terminals. *Proc. Natl. Acad. Sci. USA* 93, 331–335.
- De Camilli, P., and Takei, K. (1996). Molecular mechanisms in synaptic vesicle endocytosis and recycling. *Neuron* 16, 481–486.
- Ferro-Novick, S., and Novick, P. (1993). The role of GTP-binding proteins in transport along the exocytic pathway. *Annu. Rev. Cell Biol.* 9, 575–599.
- Garner, C.C., and Kindler, S. (1996). Synaptic proteins and the assembly of synaptic junctions. *Trends Cell Biol.* 6, 431–435.
- Geppert, M., Goda, Y., Stevens, C.F., and Südhof, T.C. (1997). Rab3A regulates a late step in synaptic vesicle fusion. *Nature* 387, 810–814.
- Gotow, T., Miyaguchi, K., and Hashimoto, P.H. (1991). Cytoplasmic architecture of the axon terminal: filamentous strands specifically associated with synaptic vesicles. *Neuroscience* 40, 587–598.
- Hanson, P.I., Heuser, J.E., and Jahn, R. (1997). Neurotransmitter release—four years of SNARE complexes. *Curr. Opin. Neurobiol.* 7, 310–315.
- Hashida, H., Goto, J., Zhao, N., Takahashi, N., Hirai, M., Kanazawa, I., and Sakaki, Y. (1998). Cloning and mapping of ZNF231, a novel brain-specific gene encoding neuronal double zinc finger protein whose expression is enhanced in a neurodegenerative disorder, multiple system atrophy (MSA). *Genomics* 54, 50–58.
- Hess, S.D., Doroshenko, P.A., and Augustine, G.J. (1993). A functional role for GTP-binding proteins in synaptic vesicle cycling. *Science* 259, 1169–1172.
- Hirokawa, N., Sobue, K., Kanda, K., Harada, A., and Yorifuji, H. (1989). The cytoskeletal architecture of the presynaptic terminal and molecular structure of synapsin 1. *J. Cell Biol.* 108, 111–126.
- Jin, M., Saucan, L., Farquhar, M.G., and Palade, G.E. (1996). Rab1a and multiple other rab proteins are associated with the transcytotic pathway in rat liver. *J. Biol. Chem.* 271, 30105–30113.
- Kotake, K., Ozaki, N., Mizuta, M., Sekiya, S., Inagaki, N., and Seino, S. (1997). Noc2, a putative zinc finger protein involved in exocytosis in endocrine cells. *J. Biol. Chem.* 272, 29407–29410.
- Kozak, M. (1987). At least six nucleotides preceding the AUG initiator codon enhance translation in mammalian cells. *J. Mol. Biol.* 196, 947–950.
- Kuhlendahl, S., Spangenberg, O., Konrad, M., Kim, E., and Garner, C.C. (1998). Functional analysis of the guanylate kinase-like domain in the synapse-associated protein SAP97. *Eur. J. Biochem.* 252, 305–313.
- Landis, D.M., Hall, A.K., Weinstein, L.A., and Reese, T.S. (1988). The organization of cytoplasm at the presynaptic active zone of a central nervous system synapse. *Neuron* 1, 201–209.
- Langnaese, K., Seidenbecher, C., Wex, H., Seidel, B., Hartung, K., Appeltauer, U., Garner, A., Voss, B., Mueller, B., Garner, C.C., and Gundelfinger, E.D. (1996). Protein components of a rat brain synaptic junctional protein preparation. *Brain Res. Mol. Brain Res.* 42, 118–122.
- Li, C., Takei, K., Geppert, M., Daniell, L., Stenius, K., Chapman, E.R., Jahn, R., De Camilli, P., and Südhof, T.C. (1994). Synaptic targeting of rabphilin-3A, a synaptic vesicle Ca<sup>2+</sup>/phospholipid-binding protein, depends on rab3A/3C. *Neuron* 13, 885–898.
- Lonart, G., Janz, R., Johnson, K.M., and Südhof, T.C. (1998). Mechanism of action of rab3A in mossy fiber LTP. *Neuron* 21, 1141–1150.
- Lupas, A. (1996). Coiled coils: new structures and new functions. *Trends Biochem. Sci.* 21, 375–382.
- Martincic, I., Peralta, M.E., and Ngsee, J.K. (1997). Isolation and characterization of a dual prenylated rab and VAMP2 receptor. *J. Biol. Chem.* 272, 26991–26998.
- Meng, X., Lu, X., Li, Z., Green, E.D., Massa, H., Trask, B.J., Morris, C.A., and Keating, M.T. (1998). Complete physical map of the common deletion region in Williams syndrome and identification and characterization of three novel genes. *Hum. Genet.* 103, 590–599.
- Morris, C.A., Demsey, S.A., Leonard, C.O., Dilts, C., and Blackburn, B.L. (1988). Natural history of Williams syndrome: physical characteristics. *J. Pediatr.* 113, 318–326.
- Müller, B.M., Kistner, U., Kindler, S., Chung, W.J., Kuhlendahl, S., Fenster, S.D., Lau, L.F., Veh, R.W., Haganir, R.L., Gundelfinger, E.D., and Garner, C.C. (1996). SAP102, a novel postsynaptic protein that interacts with NMDA receptor complexes in vivo. *Neuron* 17, 255–265.
- Nagase, T., Ishikawa, K., Miyajima, N., Tanaka, A., Kotani, H., Nomura, N., and Ohara, O. (1998). Prediction of the coding sequences of unidentified human genes. IX. The complete sequences of 100 new cDNA clones from brain which can code for large proteins in vitro. *DNA Res.* 5, 31–39.
- Ostermeier, C., and Brunger, A.T. (1999). Structural basis of Rab effector specificity: crystal structure of the small G protein Rab3A complexed with the effector domain of rabphilin-3A. *Cell* 96, 363–374.

- Pieribone, V.A., Shupliakov, O., Brodin, L., Hilfiker-Rothenfluh, S., Czernik, A.J., and Greengard, P. (1995). Distinct pools of synaptic vesicles in neurotransmitter release. *Nature* 375, 493–497.
- Qualmann, B., Roos, J., DiGregorio, P.J., and Kelly, R.B. (1999). Syndapin I, a synaptic dynamin-binding protein that associates with the neural Wiskott-Aldrich syndrome protein. *Mol. Biol. Cell* 10, 501–513.
- Richter, K., Langnaese, K., Kreutz, M.R., Olias, G., Zhai, R., Scheich, H., Garner, C.C., and Gundelfinger, E.D. (1999). The presynaptic cytomatrix protein Bassoon occurs at both excitatory and inhibitory synapses of rat brain. *J. Comp. Neurol.* 408, 437–448.
- Ringstad, N., Nemoto, Y., and De Camilli, P. (1997). The SH3p4/Sh3p8/SH3p13 protein family: binding partners for synaptojanin and dynamin via a Grb2-like Src homology 3 domain. *Proc. Natl. Acad. Sci. USA* 94, 8569–8574.
- Roos, J., and Kelly, R.B. (1998). Dap160, a neural-specific Eps15 homology and multiple SH3 domain-containing protein that interacts with *Drosophila* dynamin. *J. Biol. Chem.* 273, 19108–19119.
- Sanchez-Garcia, I., and Rabbitts, T.H. (1994). The LIM domain: a new structural motif found in zinc finger-like proteins. *Trends Genet.* 10, 315–320.
- Shirataki, H., Kaibuchi, K., Sakoda, T., Kishida, S., Yamaguchi, T., Wada, K., Miyazaki, M., and Takai, Y. (1993). Rabphilin-3A, a putative target protein for smg p25A/rab3A p25 small GTP-binding protein related to synaptotagmin. *Mol. Cell. Biol.* 13, 2061–2068.
- Südhof, T.C. (1995). The synaptic vesicle cycle: a cascade of protein-protein interactions. *Nature* 37, 645–653.
- Südhof, T.C., and Rizo, J. (1996). Synaptotagmins: C2-domain proteins that regulate membrane traffic. *Neuron* 17, 379–388.
- Sugita, S., Hata, Y., and Südhof, T.C. (1996). Distinct Ca<sup>2+</sup>-dependent properties of the first and second C2-domains of synaptotagmin I. *J. Biol. Chem.* 271, 1262–1265.
- tom Dieck, S., Sanmarti-Vila, L., Langnaese, K., Richter, K., Kindler, S., Soyke, A., Wex, H., Smalla, K.H., Kaempf, U., Franzer, J.T., et al. (1998). Bassoon, a novel zinc finger CAG/Glutamine-repeat protein selectively localized at the active zone of presynaptic nerve terminals. *J. Cell Biol.* 142, 499–509.
- Wang, Y., Okamoto, M., Schmitz, F., Hofmann, K., and Südhof, T.C. (1997). RIM is a putative Rab3 effector in regulating synaptic-vesicle fusion. *Nature* 388, 593–598.
- Winter, C., tom Dieck, S., Bockmann, J., Boeckers, T., Kaempf, U., Sanmarti-Vila, L., Langnaese, K., Altmann, W., Stumm, M., Soyke, A., et al. (1999). The presynaptic cytomatrix protein Bassoon: sequence and chromosomal localization of the human BSN gene. *Genomics* 57, 389–397.
- Yamabhai, M., Hoffman, N.G., Hardison, N.L., McPherson, P.S., Castagnoli, L., Cesareni, G., and Kay, B.K. (1998). Intersectin, a novel adaptor protein with two EH and five SH3 domains. *J. Biol. Chem.* 273, 31401–31407.
- Ye, Z., and Sontheimer, H. (1998). Astrocytes protect neurons from neurotoxic injury by serum glutamate. *Glia* 22, 237–248.

#### GenBank Accession Number

The nucleotide sequence reported in this paper has been submitted to the GenBank/EMBL Data Bank with accession number AF138789.